

X-ray signature of antistars in the Galaxy

A.E. Bondar,^a **S.I. Blinnikov,**^{b,c} **A.M. Bykov,**^d **A.D. Dolgov,**^e
K.A. Postnov^{c,e,1}

^aBudkerINP, Lavrentieva 11, Novosibirsk, 630090, Russia

^bNRC “Kurchatov institute” - ITEP, B. Cheremushkinskaya 25, 117218, Moscow, Russia

^cSternberg Astronomical Institute, M.V. Lomonosov Moscow State University,
13, Universitetskij pr., 119234, Moscow, Russia

^dIoffe Institute, Politehnicheskaya 26, St Petersburg

^eDepartment of Physics, Novosibirsk State University,
Pirogova 2, 630090, Novosibirsk, Russia

E-mail: pk@sai.msu.ru, byk@astro.ioffe.ru, dolgov@fe.infn.it

Abstract. The existence of macroscopic objects from antimatter (antistars) is envisaged in some models of baryogenesis. Searches for antistars have been usually carried out in gamma-rays originated from hadronic annihilation of matter. In astrophysically plausible cases of the interaction of neutral atmospheres or winds from antistars with ionized interstellar gas, the hadronic annihilation will be preceded by the formation of excited $p\bar{p}$ and $He\bar{p}$ atoms. These atoms rapidly cascade down to low levels prior to annihilation giving rise to a series of narrow lines which can be associated with the hadronic annihilation gamma-ray emission. The most significant are L (3p-2p) 1.73 keV line (yield more than 90%) from $p\bar{p}$ atoms, and M (4-3) 4.86 keV (yield $\sim 60\%$) and L (3-2) 11.13 keV (yield about 25%) lines from $^4He\bar{p}$ atoms. These lines can be probed in dedicated observations by forthcoming sensitive X-ray spectroscopic missions XRISM and *Athena* and in wide-field X-ray surveys like SRG/*eROSITA* all-sky survey.

¹Corresponding author.

Contents

1	Introduction	1
2	Line emissions from protonium decays	2
3	keV X-ray emission from protonium cascades in Galactic antistar candidates	4
4	Associated e^+e^- emission and optical lines	4
5	Helium-antiproton and antihelium-proton cascade X-ray lines from antistars	5
6	Possible astrophysical sources	5
7	Constraints from electron-positron annihilations	7
8	Conclusion	8

1 Introduction

According to the accepted conviction, the universe in our neighborhood consists solely of matter, and the existence of macroscopically large antimatter objects is absolutely excluded. This is in accordance with the conventional picture that the excess of baryons over antibaryons in the Universe is generated by Sakharov's mechanism [1]. In the models with explicit C and CP violation, the baryon asymmetry

$$\eta = (N_B - N_{\bar{B}})/N_\gamma \approx 6 \cdot 10^{-10} \quad (1.1)$$

is a universal constant over the whole universe. Here N_B ($N_{\bar{B}}$) are the number densities of baryons or antibaryons, and $N_\gamma = 411/\text{cm}^3$ is the current number density of photons in the cosmic microwave background (CMB) radiation.

If the charge symmetry is broken spontaneously, then domains of matter and antimatter may exist but the size of domains is expected to be cosmologically large, at the Gigaparsec level [2]. Therefore, the accepted faith is that if even macroscopically large objects or regions consisting of antimatter exist, they should be far away from us at the edge of the universe or at least at distances beyond 10 Mpc [3].

On the other hand, about a quarter of century ago, a physical mechanism was suggested leading to the possible formation of compact antistars over normal matter-dominated background [4, 5]. According to the proposed scenario, the baryogenesis in the bulk of the universe proceeded in the usual way giving rise to the observed small baryon asymmetry (1.1), while in a small by volume part of the universe, bubbles with a very high baryonic number (called HBB) might be created. The model allows for the formation of HBBs with both signs of the baryon asymmetry, positive (matter) and negative (antimatter). HBBs with size comparable to the cosmological horizon at the QCD (quantum chromodynamics) phase transition at $T \sim 100$ MeV mostly give rise to primordial black holes (PBHs) which could make a sizeable fraction (if not all) of cosmological dark matter. Such PBHs could have masses in a wide range from a fraction of solar mass to thousands solar masses [6, 7]. Of course, there is no noticeable difference between a PBH and an anti-PBH.

Smaller HBBs could form compact stars or antistars. They would be created in the very early universe after the QCD phase transition at $T \sim 100$ MeV. Probably, they can be now observed as

peculiar stars in the Galaxy: too old stars, very fast-moving stars, and stars with a highly unusual chemical content [8–10], for a review see [11]. They should also populate the galactic halo. The fraction of these strange stars and/or antistars among the stellar population is model-dependent but may be quite high.

The possibility of the existence of a population of antistars in the Galaxy and observational limits on their density were analyzed in several papers [12–15]. It was concluded that quite a noticeable fraction of antistars is not excluded by the present observations.

Recently, the idea that antistars may be our Galactic neighbors attracted new attention. In ref. [16], it was suggested that cosmological dark matter could entirely consist of macroscopic antimatter objects, and in ref. [17] a possible indication to antistars in the Galaxy was reported. Quoting the latter paper: “We identify in the catalog 14 antistar candidates not associated with any objects belonging to established gamma-ray source classes and with a spectrum compatible with baryon-antibaryon annihilation.”

Usually, the antimatter objects are being looked for through the search for energetic photons with energies of hundreds MeV from π^0 decays into two gamma-photons, with π^0 emerging from $p\bar{p}$ -annihilation. The energy spectrum of such photons is shown in Fig.1. This spectrum was calculated by Geant4¹ [18] simulation of the low-energy antiproton annihilation in a small liquid hydrogen target. Note that the target material and structure do not significantly affect the annihilation spectrum which is appropriate for the considered problem.

In this paper, we propose a new signature tagging electromagnetic signal from annihilation in outer layers of antistars. The idea is to search for antistars in the Galaxy through X-rays in the $\sim (1 - 10)$ keV energy band. This X-ray radiation is expected to be produced in the process of the cascade transition from bound states of antiproton-proton (protonium) or antihelium-proton atoms prior to $p\bar{p}$ -annihilation and must accompany the gamma-ray radiation from the annihilation.

2 Line emissions from protonium decays

Prior to annihilation, protons and antiprotons could form atomic-type excited bound states (‘protonium’, Pn), similar to e^+e^- -positronium (Ps) atoms. One could expect that in the process of de-excitation of Pn, an antistar could emit not only ~ 100 -MeV gamma-rays but a noticeable flux of X-rays with energies in the keV range.

Let us briefly remind the basic physics of $p\bar{p}$ annihilation through a protonium state (see, e.g. [19] for a comprehensive review). A protonium atom can form during the interaction of p with neutral (or molecular) antimatter. In the ionized matter-antimatter interaction, the annihilation mainly proceeds through the direct hadronic channel, the cross-section of the radiative recombination of a Pn atom formation from the $p\bar{p}$ interaction being $(m_e/m_p)^{3/2} \approx 10^{-5}$ times smaller (see [3] for the matter-antimatter annihilation cross-sections).

A Pn atom forms when a proton (antiproton) interacts with an anti-hydrogen (hydrogen) atom, $\bar{p} + H \rightarrow (p, \bar{p}) + e^-$. The formation of a Pn atom effectively occurs when the energy of the proton in the lab frame is below the electron’s ionization threshold in atomic hydrogen, $E = 1\text{Ry} \approx 13.6$ eV. At lower proton energies, the cross-section increases as $\sim 1/\sqrt{E}$ [20]. Therefore, in the present paper we will mainly focus on astrophysical situations where the antistar’s atmosphere (or its stellar wind) is neutral or interacts with neutral interstellar medium (ISM).

The fraction of energy from the bolometric luminosity released in X-ray from the Pn cascades (the cascade yield), $f_X = L_X(Pn)/L_a$, depends on the pressure [21]. However, an upper limit on

¹version Geant4.10.06 (06.12.2019); <https://geant4.web.cern.ch>

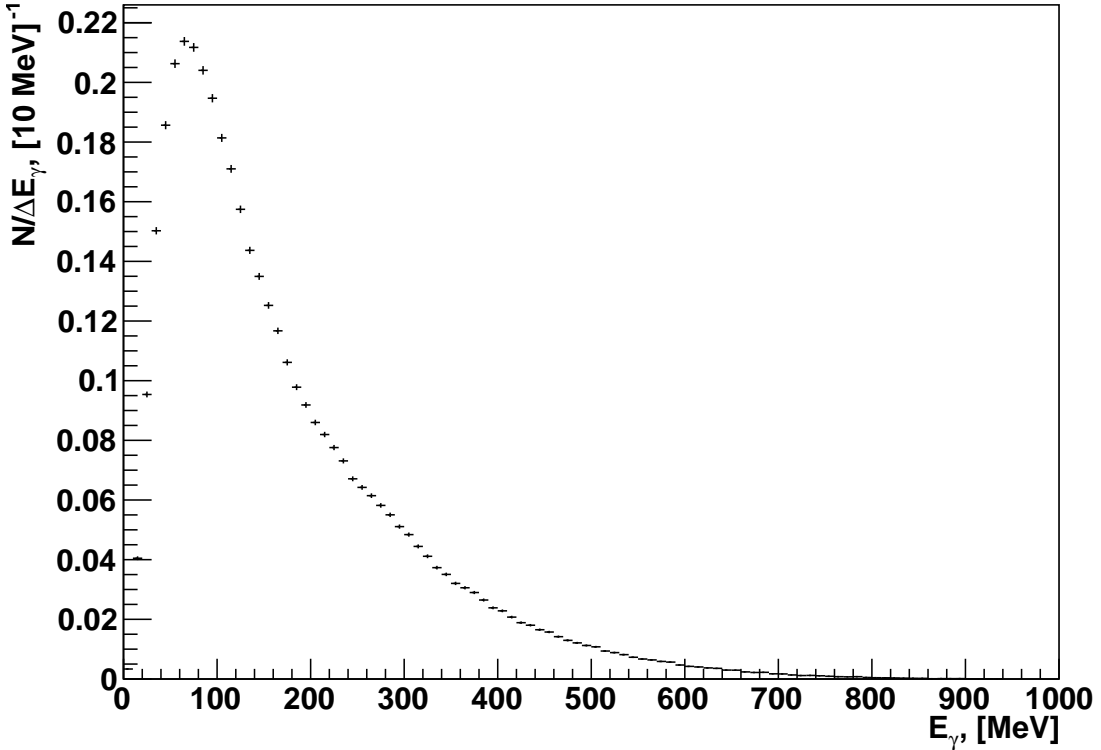


Figure 1. Gamma-ray spectrum from hadronic $p\bar{H}$ annihilation. The mean number of γ -quanta per event is $\langle N_\gamma \rangle \geq 4.12$. The mean number of γ -quanta above 100 MeV is 2.63 per event. The mean energy radiated in gamma-rays per one annihilation is $\Delta E_\gamma = 617.5$ MeV. Calculations by Geant4 code.

the bolometric X-ray yield per unit cascade can be estimated as the binding energy of a Pn atom, ≈ 12.5 keV (ignoring small QED corrections $O(\alpha^2)$). Therefore, the maximum X-ray yield per one Pn atom is $R_{p\bar{p}} = 1/4m_p\alpha^2c^2 = 12.5$ keV (α is the fine structure constant, m_p is proton's mass). As the cascade time of a Pn atom is very short [21], in rarefied media the X-ray luminosity in X-ray lines will be determined by the formation rate of Pn atoms, \dot{N}_a : $L_X \leq 12.5 \text{ keV} \times \dot{N}_a$, i.e. the maximum possible X-ray fraction in the Pn-cascade during matter-antimatter annihilation is $f_{X,\text{max}} = \alpha^2/8 \approx 6.7 \times 10^{-6}$.

The line energies for the K (Lyman) $2p \rightarrow 1s$, L (Balmer) $3d \rightarrow 2p$ and M (Paschen) $4f \rightarrow 3d$ transitions in a Pn atom are 9409 eV, 1737 eV and 607 eV, respectively. Calculations of the X-ray line yields from the Pn decays produced in $p\bar{H}$ interactions at low densities [22] suggest that most intensive X-ray lines should be Balmer (L) lines (up to 97%), the 2p-states of the $p\bar{p}$ atom being rapidly annihilated. The produced X-ray line width is determined by the $p\bar{p}$ annihilation from the 2p-state and is about $\Delta E \sim O(0.1 \text{ eV})$ (see the discussion and experimental measurements in [19]). As the total energy released in gamma-rays during $p\bar{H}$ annihilation is about 617 MeV (see Fig. 1), the expected fraction of X-ray line emission flux from one Pn annihilation is $f_X \approx 0.95 \times (1.7 \text{ keV}/617.5 \text{ MeV}) \approx 2.5 \times 10^{-6}$, i.e. a factor of three lower than the simple estimate given above.

3 keV X-ray emission from protonium cascades in Galactic antistar candidates

Presently, it is difficult to reliably assess the number and physical parameters of antistars in the Galaxy. Estimates in paper [10] are model-dependent and based on the assumption that gamma-ray emission from hadronic annihilation occurs in antistars during Bondi-Hoyle-Littleton accretion of the interstellar gas. It is straightforward to estimate the expected X-ray flux associated with the gamma-ray annihilation emission in the case where the $p\bar{p}$ annihilation was preceded by the protonium formation.

A crude estimate of the X-ray flux emitted in 1.7-keV narrow line from the gamma-ray sources – candidates to antistars found from *Fermi* 10-year LAT catalogue in ref. [17] is:

$$F_X(1.7 \text{ keV}) \sim F_\gamma \left(\frac{E_X}{E_\gamma} \right) \sim 3 \times 10^{-17} [\text{erg cm}^{-2}\text{s}^{-1}] \left(\frac{F_\gamma(0.1 - 100 \text{ GeV})}{3 \times 10^{-12} \text{ erg cm}^{-2}\text{s}^{-1}} \right) \left(\frac{E_X}{1.7 \text{ keV}} \right) \left(\frac{200 \text{ MeV}}{E_\gamma} \right)$$

In fact, this is an upper limit considering that one 1.7 keV photon is, on average, emitted per three gamma-quanta with energy $E_\gamma \approx 200$ MeV released from $\pi^0 \rightarrow \gamma + \gamma$ emission (see Fig. 1). This low flux is unlikely to be detected with the current instrumentation.

The forthcoming JAXA/NASA XRISM (X-Ray Imaging and Spectroscopy Mission) telescope will be able to provide a 5-4 eV resolution in the 0.3-12 keV energy range [23]. The expected effective area of the *Resolve* spectrometer is $\sim 210 \text{ cm}^2$ ². For a $\sim 1 \text{ Ms}$ observations, only a few 2-keV photons from a source with X-ray flux $\sim 3 \times 10^{-17} \text{ erg cm}^2 \text{ s}^{-1}$ can be collected. A more promising could be measurements from the ATHENA X-IFU X-ray spectrometer which is expected to have a spectral resolution of $\sim 2 \text{ eV}$ and an effective area of $\sim 8000 \text{ cm}^2$ in the keV range [24, 25].

4 Associated e^+e^- emission and optical lines

During the formation of a Pn atom from the interaction of a proton with \bar{H} in the upper atmosphere of an antistar, a slow positron e^+ is ejected. It should form a positronium e^+e^- atom in the surrounding medium before annihilation. Since during the Pn cascade transitions and annihilation, on average, three gamma-quanta with energy $E_\gamma \approx 200$ MeV are created per 600 MeV, the number of the accompanying e^+e^- annihilation flux from the *Fermi* antistar candidates is:

$$\frac{dN}{dAdt} \Big|_{e^+e^-} \approx 2 \times \frac{1}{3} \frac{dN}{dAdt} \Big|_\gamma \approx 6 \times 10^{-9} \frac{\text{ph}}{\text{cm}^2\text{s}} \left(\frac{F_\gamma(0.1 - 100 \text{ GeV})}{3 \times 10^{-12} \text{ erg cm}^{-2}\text{s}^{-1}} \right) \left(\frac{200 \text{ MeV}}{E_\gamma} \right). \quad (4.1)$$

(The factor 2 above is due to at least two photons are emitted in the Ps annihilation). This is much smaller than the current 511 keV detection capabilities [26].

Another possible traces of the Pn atom cascade decays could be searched for in the optical-UV range. Indeed, a Pn bound state is expected to be form highly excited, $n \gtrsim 30$ [19]. The Pn energy levels are

$$E_n \approx -\frac{12.5}{n^2} \text{ keV} = -0.93 \text{ eV} \left(\frac{30}{n} \right)^2, \quad (4.2)$$

and the cascade transitions $(n, l = n - 1) \rightarrow (n - 1, l - 2)$ pass through the optical-UV range. Clearly, the number of quanta in an optical emission line from the *Fermi* antistar candidates should be approximately equal to the number of Pn atoms, therefore $\frac{dN}{dAdt} \Big|_{\text{opt}} \approx \frac{dN}{dAdt} \Big|_\gamma \approx 3 \times 10^{-9} \frac{\text{ph}}{\text{cm}^2\text{s}}$.

This photon flux in the optical line corresponds to a faint source of $\sim 29^m$ visual magnitude. The spacing of the optical lines is $\Delta E/E = \Delta\lambda/\lambda = 2/n$ is much larger than their expected Doppler width, which could be a distinctive feature of such lines.

²<https://xrism.isas.jaxa.jp/research/documents/index.html>

5 Helium-antiproton and antihelium-proton cascade X-ray lines from antistars

An enhanced production of helium and metals is an important feature of the non-standard nucleosynthesis in HBBs with high η [8–10]. Therefore, it is instructive to consider the X-ray lines arising from cascade decays of ${}^4\bar{\text{He}}\text{p}$ and ${}^4\text{He}\bar{\text{p}}$ atoms that can be created in interaction of ISM with antistars. The possible AMS-02 detection of non-thermal antihelium-4 nuclei³ may indicate the presence of antistars in the Galaxy because its secondary production in the universe is challenging (see, e.g., the discussion in [27]). Note that the magnetically active antistars may accelerate antihelium nuclei in stellar flares.

In a ${}^4\text{He}\bar{\text{p}}$ atom, the hadronic annihilation starts dominating the cascade transitions already at the third level. The ${}^4\text{He}\bar{\text{p}}$ atom transitions series M (4-3) at 4.86 keV [yield $(57 \pm 3)\%$] and L (3-2) 11.13 keV [yield $(25 \pm 5)\%$] [28] are certainly of interest given that the forthcoming X-ray spectroscopic mission *XRISM* [29] is sensitive in 0.3–12 keV energy range. These lines can be even more important from the observational viewpoint because the protonium $p\bar{p}$ 3d-2p transition line energy 1.73 keV is close to the Si K-shell complex lines and, therefore, a high energy resolution is needed to distinguish the lines.

Note also that in a medium with ionized hydrogen, when protonium atoms will not be formed, even a small mixture of He^+ ions would give rise to the effective (with atomic cross-sections) formation of $\text{He}\bar{\text{p}}$ atoms. Then only ${}^4\text{He}\bar{\text{p}}$ cascade X-ray lines will be produced.

A dedicated search for ${}^4\text{He}\bar{\text{p}}$ 4.86 keV and 11.13 keV lines in all-sky surveys like *Spectrum-RG* [30] could also constrain the collective contribution of X-ray emission from antistars with enhanced He abundance.

Like in the case of antiprotonium, ${}^4\text{He}\bar{\text{p}}$ atoms are formed at excited levels with principal numbers $28 < n < 35$. After the antiproton is captured, the remaining electron is rapidly ejected due to the internal Auger effect, and the process of ion $({}^4\text{He}\bar{\text{p}})^+$ radiative deexcitation begins along the circular sequence from $n \sim 30$ [31]. Neglecting the strong interaction shift, the energy between consequent levels is

$$\Delta E_n \approx 3.72 \text{ eV} \left(\frac{30}{n} \right)^2 \frac{2n-1}{(n-1)^2}, \quad (5.1)$$

and these lines can be probed in the optical range too.

6 Possible astrophysical sources

As shown above, it is challenging to test the Pn formation before hadronic annihilation in the *Fermi* Galactic antistar candidates. However, there could be favorable astrophysical conditions for Pn creation from the interaction of antistars with ISM.

Consider first an antistar with mass M and the standard (solar) abundance residing in the Galactic ISM with density ρ_0 (or number density n_0) and moving with the velocity v . There can be distinct cases of the star's interaction with the ISM depending on the evolutionary state of the antistar (main-sequence or evolved) and its velocity.

If the star is on the main sequence and has an insignificant mass-loss via stellar wind, the interaction with the ISM will be characterized by the gravitationally captured mass-rate (the Bondi-Hoyle-Littleton accretion). The relevant physical size is the Bondi radius,

$$R_B = \frac{2GM}{(v^2 + c_s^2)} \quad (6.1)$$

³S. Ting, Latest Results from the AMS Experiment on the International Space Station (2018)

where v and c_s is the star's velocity and ISM sound speed, respectively, G is the Newtonian gravitational constant. The Bondi mass accretion rate is

$$\dot{M}_B = \pi R_B^2 \rho_0 \sqrt{v^2 + c_s^2} \quad (6.2)$$

If a star has significant proper mass-loss rate \dot{M}_w , the interaction with ISM will be characterized by the radius R_w , where the dynamical pressure of the stellar wind is balanced by the ISM pressure, $\rho_w v_w^2 \sim \rho_0 c_s^2$:

$$R_w = \sqrt{\frac{\dot{M}_w (v_w/c_s)}{4\pi \rho_0 c_s}} \quad (6.3)$$

If $R_w > R_B$, the ISM accretion is insignificant and the stellar wind directly interacts with ISM.

Several cases can be distinguished.

1. Low-velocity case, low stellar wind $v \lesssim c_{\text{ISM}} \sim 10 \text{ km s}^{-1}$, $\dot{M}_w \approx 0$

In this case, the Bondi radius is $R_B \approx 2 \times 10^{14} [\text{cm}] m v_6^{-2} \approx 2.7 \times 10^3 R_\odot v_6^{-2}$ (here $m \equiv (M/M_\odot)$, $v_6 \equiv v/(10^6 \text{ cm s}^{-1})$, $R_\odot \approx 7 \times 10^{10} \text{ cm}$ is the solar radius). The BHL accretion rate from ISM onto such a star is $\dot{M}_B \approx 1.8 \times 10^{11} [\text{g s}^{-1}] m^2 v_6^{-3}$. The total annihilation rate is thus $\dot{N}_a \sim 10^{35} \text{ s}^{-1}$ and the bolometric annihilation luminosity is $L_a \sim 2 \text{ GeV} \times \dot{N}_a \sim 3 \times 10^{32} \text{ erg s}^{-1}$. The maximum possible Pn-cascade X-ray luminosity is then $L_X = \alpha^2/8 \times L_a \approx 2 \times 10^{27} [\text{erg s}^{-1}] m^2 v_6^{-3}$.

2. Low-velocity case, strong stellar wind $v \lesssim c_{\text{ISM}} \sim 10 \text{ km s}^{-1}$, $\dot{M}_w \approx 10^{-6} M_\odot \text{ yr}^{-1}$.

This can be the case of a red (super)giant antistar at a late evolutionary stage. Here $R_w \approx 2.2 \times 10^{18} [\text{cm}] \dot{M}_{w,-6}^{1/2} n_0^{-1/2} (v_w/c_s)^{1/2} \gg R_B$. Here $M_{w,-6} \equiv \dot{M}_w/(10^{-6} M_\odot \text{ yr}^{-1})$. The cross-section of Pn formation under these conditions is about 10^{-16} cm^2 [20]. The formation of Pn states occurs in a layer with a width of $\sim 1/(n_0 \sigma) \sim 10^{16} \text{ cm} \ll R_w$. The Pn formation rate is $\dot{N}_a = \dot{M}_w/m_p \text{ s}^{-1}$ suggesting a bolometric annihilation luminosity of $L_a \sim 10^{41} [\text{erg s}^{-1}] \dot{M}_{w,-6}$. The Pn-cascade X-ray luminosity is $L_X \lesssim 6.7 \times 10^{35} [\text{erg s}^{-1}] \dot{M}_{w,-6}$. This estimate holds insofar as $R_w > R_B$.

3. High-velocity case, $v \gg c_{\text{ISM}} \sim 10 \text{ km s}^{-1}$, weak stellar wind $\dot{M}_w \approx 0$.

This case is more relevant if antistars populate the Galactic halo and move with the halo virial velocities $v \sim 10^{-3} c$ (c is the speed of light). In this case, the Bondi radius is very small, $R_B \sim 4 R_\odot v_{-3}^{-2}$ (here $v_{-3} = 10^{-3} (v/c)$), the BHL accretion is inefficient, $\dot{M}_B \sim 10^7 [\text{g s}^{-1}] m^2 n_0 v_{-3}^{-3}$, the associated annihilation luminosity is very weak.

4. High-velocity case, $v \gg c_{\text{ISM}} \sim 10 \text{ km s}^{-1}$, strong stellar wind $\dot{M}_w \approx 10^{-6} M_\odot \text{ yr}^{-1}$.

If an evolved antistar with strong stellar wind moves with the virial velocity through ISM, $v_{-3} \sim 1$, a strong bow shock is formed ahead of the star. The matter behind the shock front is fully ionized. The front shock radius is estimated from the dynamical wind pressure balance: $R_{sh} = \sqrt{\dot{M} v_w / (4\pi \rho_0 v^2)} \simeq 7 \times 10^{16} [\text{cm}] \dot{M}_{w,-6}^{1/2} \rho_{-24}^{-1/2} v_6^{1/2} \beta_{-3}^{-1}$, where $\beta = v/c$ is the star's velocity in units of the speed of light, $\rho_{-24} = \rho/(10^{-24} \text{ g cm}^{-3})$ is the ISM density. The flow of matter with a downstream velocity of $v_p \approx (1/4)v_{sh}$ interacts with the stellar wind.

This case is more complicated than the interaction of a cold slow stellar wind with ISM. The energy of protons downstream the shock is $E_p = m_p v_p^2/2 \sim 32 \text{ eV}$. In this case, the direct annihilation cross-section is roughly $\sigma \sim 10^{-23} \text{ cm}^2$ [3], and the protons penetrate much deeper into the stellar wind before annihilating through the hadronic channel. The cross-section of Pn

formation strongly depends on the proton's energy and below $\sim \text{Ry} \sim 13.6 \text{ eV}$ sharply increases up to a few $\times 10^{-16} \text{ cm}^2$. However, the protons rapidly loose energy by interacting with neutral stellar wind. The proton stopping length in hydrogen is [M.J. Berger et al. 1993 ICRU Report 49]

$$l = \frac{E_p}{dE_p/dx} = \frac{E_p}{4\pi r_e^2 m_e c^2 \beta_p^{-2} (\rho_w/m_p) L(\beta)} \quad (6.4)$$

Here $\beta_p = v_p/c$ is the proton's downstream velocity, $L(\beta_p)$ is the proton's stopping number. For low proton energies, it can be evaluated only from experiments, and is dominated by nuclear scatterings. For an estimate of the stopping length of slow protons, we can use the ionization energy loss of slow protons in electron gas $L(\beta_p) \approx \log(2m_e v^2/\hbar\omega_0)$, where $\omega_0 \approx 5.6 \times 10^4 \sqrt{n_e} \text{ rad s}^{-1}$ is the electron plasma frequency [32]. Then $l \lesssim 10^{12} [\text{cm}] (\beta_p/(4 \times 10^{-3}))^4$, which is much smaller than the shock front radius R_{sh} . Therefore, the ISM protons are expected to form Pn atoms inside the wind in analogy with the low-velocity case considered above.

If a typical antistar has an atmosphere like that of our Sun, then modeling by Kurucz's ATLAS code⁴ shows that the bulk of proton annihilations takes place in essentially neutral plasma. Then the data on antiproton annihilations in laboratory neutral media are quite applicable for proton annihilations in Solar-like atmospheres of antistars. Different possible atmospheric structures of antistars or their coronas deserve a special investigation.

7 Constraints from electron-positron annihilations

The interaction of an antistar with ISM should be necessarily accompanied with electron-positron annihilation. Therefore, the existing observations of the e^+e^- Galactic emission should be taken into account when constraining the possible Galactic antistar populations.

The characteristic 511 keV annihilation radiation from the Milky Way was discovered about 50 years ago in balloon-borne experiments. Since then it has been measured by a number of space missions [see for a review 33, 34]. The recent analysis of *INTEGRAL SPI* Ge detector data [26] has confirmed the presence of the main extended 511 keV components with a total significance of about 58σ . The 511 keV fluxes estimations depend on the models of the extended Galactic emission. The total 511 keV flux from the Milky Way was estimated to be $(2.74 \pm 0.25) \times 10^{-3} \text{ ph cm}^{-2} \text{ s}^{-1}$. The bulge component contributed about $(0.96 \pm 0.07) \times 10^{-3} \text{ ph cm}^{-2}$, and the 511 keV flux ratio of the bulge to disk components was derived to be (0.58 ± 0.13) .

The total 511 keV Galactic disk emission suggests an annihilation flux of $F_{e^+e^-} \sim 2 \times 10^{-3} \text{ cm}^{-2} \text{ s}^{-1}$. For a fiducial distance of 10 kpc this rate corresponds to a total positron production $\dot{N}_{e^+e^-} \sim 10^{43} \text{ s}^{-1}$. If all positrons were formed in Pn $p\bar{p}$ annihilations in a purely hydrogen matter, the upper limit on the protonium production rate would be $\dot{N}_{\text{Pn}} \sim 10^{43} \text{ s}^{-1}$, corresponding to $\sim 2 \times 10^{-7} M_\odot \text{ yr}^{-1}$. Therefore, an antistar with higher wind mass-loss rate is excluded by the e^+e^- Galactic emission.

Recently, ref. [35] reported an improved INTEGRAL upper limit on the 511-keV flux from the Galactic satellite dwarf galaxy Ret II of $F_{511} < 1.7 \times 10^{-4} \text{ ph cm}^{-2} \text{ s}^{-1}$. Given the distance 30 kpc to this galaxy, this flux is translated to an e^+e^- annihilation rate of about $\dot{N}_{e^+e^-} \sim 10^{43} \text{ s}^{-1}$, comparable to the detected Galactic value. The gamma-ray flux in GeV range measured by Fermi-LAT from Ret II galaxy is inconclusive [36]. The authors [35] do not exclude the 511 keV flux variability on a decade-long time-scale. In the frame of the astrophysical models discussed above (i.e., the interaction of antistars with ISM), the e^+e^- -flux variability might be due to the intrinsically variable stellar wind mass-loss rate.

⁴<http://kurucz.harvard.edu/programs.html>

8 Conclusion

Antistars in the universe can be created in the modified Affleck-Dine baryogenesis mechanism [4, 5]. Presently, they could be observed as old halo stars with unusual chemical composition.

In the present paper, we explored the possibility that the interaction of antistars with ISM gas can proceed with the formation of excited protonium atoms which rapidly cascade down before hadronic annihilation from 2p-states. The formation of Pn atoms most effectively occurs during interaction of protons with neutral (or molecular) antimatter. This can happen if an antistar has a noticeable wind mass-loss. We considered the case where in analogy with ordinary stars, antistars in the mass range from ~ 0.8 to $8M_\odot$ at the end of their core nuclear burning can have cold low-velocity stellar winds $\sim 10^{-8} - 10^{-5}M_\odot \text{ yr}^{-1}$ [37, 38] (AGB antistars). The interaction of cold stellar winds from antistars with ISM can proceed through the formation of excited protonium ($p\bar{p}$) atoms. The protonium atoms cascade to the 2p-state producing mostly L (Balmer) 3d-2p X-rays around ~ 1.7 keV before the $p\bar{p}$ hadronic annihilation.

Antistars formed in HBBs should have an enhanced helium abundance. Therefore, the 4.86 keV M (4-3) and 11.13 L (3-2) narrow X-ray lines from cascade transitions in ${}^4\text{He}\bar{p}$ atoms can also be associated with gamma-rays from hadronic annihilations. These lines are interesting from the observational point of view because the protonium 3d-2p transition line energy 1.73 keV is close to the Si K-shell complex lines, which could hamper its disentangling from the background.

The expected Pn-decay X-ray line flux from individual Galactic *Fermi* antistar candidates reported in [17] is estimated to be much lower than the sensitivity of current X-ray detectors. However, searches for the cascade X-ray transitions from Pn and ${}^4\text{He}\bar{p}$ atoms associated with hadronic annihilation gamma-rays can be exciting targets for the forthcoming X-ray spectroscopic missions like *XRISM* and *Athena*. Sensitive wide-field X-ray surveys can also help to constrain the collective contribution of antistars in the universe.

Acknowledgement

We are grateful to Andrey Sokolov for his help in the simulation of the gamma-ray spectrum from hadronic $p\bar{H}$ annihilation. The work of AD and KP was supported by the RSF Grant 19-42-02004. SB acknowledges support of RSF Grant 19-12-00229 in his work on stellar atmospheres. KP thanks the Interdisciplinary Scientific Educational School of Moscow University 'Fundamental and applied space research' for support of this research.

References

- [1] A. D. Sakharov, *Violation of CP Invariance, C Asymmetry, and Baryon Asymmetry of the Universe*, *Soviet Journal of Experimental and Theoretical Physics Letters* **5** (1967) 24.
- [2] A. G. Cohen, A. De Rújula and S. L. Glashow, *A Matter-Antimatter Universe?*, *ApJ* **495** (1998) 539 [[astro-ph/9707087](#)].
- [3] G. Steigman, *Observational tests of antimatter cosmologies.*, *ARA&A* **14** (1976) 339.
- [4] A. Dolgov and J. Silk, *Baryon isocurvature fluctuations at small scales and baryonic dark matter*, *Physical Review D* **47** (1993) 4244.
- [5] A. D. Dolgov, M. Kawasaki and N. Kevlishvili, *Inhomogeneous baryogenesis, cosmic antimatter, and dark matter*, *Nuclear Physics B* **807** (2009) 229 [[0806.2986](#)].
- [6] S. Blinnikov, A. Dolgov, N. K. Porayko and K. Postnov, *Solving puzzles of GW150914 by primordial black holes*, *JCAP* **2016** (2016) 036 [[1611.00541](#)].

[7] A. Dolgov and K. Postnov, *Why the mean mass of primordial black hole distribution is close to $10M_{solar}$* , *JCAP* **2020** (2020) 063 [[2004.11669](#)].

[8] S. Matsuura, A. D. Dolgov and S. Nagataki, *Affleck-Dine Baryogenesis and Heavy Element Production from Inhomogeneous Big Bang Nucleosynthesis*, *Progress of Theoretical Physics* **112** (2004) 971 [[astro-ph/0405459](#)].

[9] S. Matsuura, S.-I. Fujimoto, S. Nishimura, M.-A. Hashimoto and K. Sato, *Heavy element production in inhomogeneous big bang nucleosynthesis*, *Physical Review D* **72** (2005) 123505 [[astro-ph/0507439](#)].

[10] A. Arbey, J. Auffinger and J. Silk, *Stellar signatures of inhomogeneous big bang nucleosynthesis*, *Physical Review D* **102** (2020) 023503 [[2006.02446](#)].

[11] A. D. Dolgov, *Massive and supermassive black holes in the contemporary and early Universe and problems in cosmology and astrophysics*, *Physics Uspekhi* **61** (2018) 115 [[1705.06859](#)].

[12] C. Bambi and A. D. Dolgov, *Antimatter in the Milky Way*, *Nuclear Physics B* **784** (2007) 132 [[astro-ph/0702350](#)].

[13] A. D. Dolgov, V. A. Novikov and M. I. Vysotsky, *How to see an antistar*, *Soviet Journal of Experimental and Theoretical Physics Letters* **98** (2014) 519 [[1309.2746](#)].

[14] A. D. Dolgov and S. I. Blinnikov, *Stars and black holes from the very early universe*, *Physical Review D* **89** (2014) 021301 [[1309.3395](#)].

[15] S. I. Blinnikov, A. D. Dolgov and K. A. Postnov, *Antimatter and antistars in the Universe and in the Galaxy*, *Physical Review D* **92** (2015) 023516 [[1409.5736](#)].

[16] J. S. Sidhu, R. J. Scherrer and G. Starkman, *Antimatter as macroscopic dark matter*, *Physics Letters B* **807** (2020) 135574 [[2006.01200](#)].

[17] S. Dupourqué, L. Tibaldo and P. von Ballmoos, *Constraints on the antistar fraction in the Solar System neighborhood from the 10-year Fermi Large Area Telescope gamma-ray source catalog*, *Physical Review D* **103** (2021) 083016 [[2103.10073](#)].

[18] J. Allison et al., *Geant4 developments and applications*, *IEEE Trans. Nucl. Sci.* **53** (2006) 270.

[19] E. Klempert, F. Bradamante, A. Martin and J.-M. Richard, *Antinucleon-nucleon interaction at low energy: scattering and protonium*, *Phys. Rep.* **368** (2002) 119.

[20] S. Y. Ovchinnikov and J. H. Macek, *Protonium formation in antiproton-hydrogen-atom collisions*, *Physical Review A* **71** (2005) 052717.

[21] G. Reifernröther and E. Klempert, *Antiprotonic hydrogen: From atomic capture to annihilation*, *Nucl. Phys. A* **503** (1989) 885.

[22] J. S. Cohen and N. T. Padial, *Initial distributions, cascade, and annihilation of $\bar{p}p$ atoms formed in $\bar{p}+H$ and $\bar{p}+H^-$ collisions in near vacuum*, *Physical Review A* **41** (1990) 3460.

[23] M. Tashiro, H. Maejima, K. Toda and R. K. et al., *Concept of the X-ray Astronomy Recovery Mission*, in *Space Telescopes and Instrumentation 2018: Ultraviolet to Gamma Ray*, J.-W. A. den Herder, S. Nikzad and K. Nakazawa, eds., vol. 10699, pp. 520 – 531, International Society for Optics and Photonics, SPIE, 2018, <https://doi.org/10.1117/12.2309455>.

[24] D. Barret, T. Lam Trong, J.-W. den Herder, L. Piro, X. Barcons, J. Huovelin et al., *The Athena X-ray Integral Field Unit (X-IFU)*, in *Space Telescopes and Instrumentation 2016: Ultraviolet to Gamma Ray*, J.-W. A. den Herder, T. Takahashi and M. Bautz, eds., vol. 9905 of *Society of Photo-Optical Instrumentation Engineers (SPIE) Conference Series*, p. 99052F, July, 2016, [1608.08105](#), DOI.

[25] D. Barret, A. Decourchelle, A. Fabian, M. Guainazzi, K. Nandra, R. Smith et al., *The Athena space X-ray observatory and the astrophysics of hot plasma*, *Astronomische Nachrichten* **341** (2020) 224 [[1912.04615](#)].

[26] T. Siegert, R. Diehl, G. Khachtryan, M. G. H. Krause, F. Guglielmetti, J. Greiner et al., *Gamma-ray spectroscopy of positron annihilation in the Milky Way*, *A&A* **586** (2016) A84 [[1512.00325](#)].

[27] V. Poulin, P. Salati, I. Cholis, M. Kamionkowski and J. Silk, *Where do the AMS-02 antihelium events come from?*, *Physical Review D* **99** (2019) 023016 [[1808.08961](#)].

[28] M. Schneider, R. Bacher, P. Blüm, D. Gotta, K. Heitlinger, W. Kunold et al., *X-rays from antiprotonic ^3He and ^4He* , *Zeitschrift fur Physik A Hadrons and Nuclei* **338** (1991) 217.

[29] XRISM Science Team, *Science with the X-ray Imaging and Spectroscopy Mission (XRISM)*, *arXiv e-prints* (2020) arXiv:2003.04962 [[2003.04962](#)].

[30] R. Sunyaev, V. Arefiev, V. Babyshkin, A. Bogomolov, K. Borisov, M. Buntov et al., *The SRG X-ray orbital observatory, its telescopes and first scientific results*, *arXiv e-prints* (2021) arXiv:2104.13267 [[2104.13267](#)].

[31] G. Reifernröther, E. Klempt and R. Landua, *Cascade of antiprotonic helium atoms*, *Physics Letters B* **203** (1988) 9.

[32] J. Lindgard, *On the properties of a gas of charge particles*, *Dan. Mat. Fys. Medd.* **28** (1954) .

[33] N. Prantzos, C. Boehm, A. M. Bykov, R. Diehl, K. Ferrière, N. Guessoum et al., *The 511 keV emission from positron annihilation in the Galaxy*, *Reviews of Modern Physics* **83** (2011) 1001 [[1009.4620](#)].

[34] E. Churazov, L. Bouchet, P. Jean, E. Jourdain, J. Knöldlseder, R. Krivonos et al., *INTEGRAL results on the electron-positron annihilation radiation and X-ray & Gamma-ray diffuse emission of the Milky Way*, *New Astron. Rev.* **90** (2020) 101548.

[35] T. Siegert, C. Boehm, F. Calore, R. Diehl, M. G. H. Krause, P. D. Serpico et al., *Reticulum II: Particle Dark Matter and Primordial Black Holes Limits*, *arXiv e-prints* (2021) arXiv:2109.03791 [[2109.03791](#)].

[36] S. Hoof, A. Geringer-Sameth and R. Trotta, *A global analysis of dark matter signals from 27 dwarf spheroidal galaxies using 11 years of Fermi-LAT observations*, *JCAP* **2020** (2020) 012 [[1812.06986](#)].

[37] T. Bloecker, *Stellar evolution of low and intermediate-mass stars. I. Mass loss on the AGB and its consequences for stellar evolution.*, *A&A* **297** (1995) 727.

[38] S. Ramstedt, F. L. Schöier, H. Olofsson and A. A. Lundgren, *On the reliability of mass-loss-rate estimates for AGB stars*, *A&A* **487** (2008) 645 [[0806.0517](#)].